Buckle Up for Buckling:

Poacher Fish Scale Behavior Under Compression

Brody Andersen[1,2], Karly Cohen[2], Katherine Corn[1], Megan Vandenberg[2], John Michael Racy[2,3], Cassandra Donatelli[2,4]

Friday Harbor Labs REU 2025

[1] Washington State University, Pullman, WA, 99163
[2] Friday Harbor Laboratories, University of Washington, Friday Harbor, WA, 98250
[3] University of Washington, Seattle, WA, 98195
[4] University of Washington, Tacoma, WA, 98402

Contact information:
Brody Andersen
School of Biological Sciences
Washington State University
1815 Wilson Rd.
Pullman WA, 99163
brody.andersen@wsu.edu

Abstract

Poacher fishes (*Agonidae*) are a family defined by their bony armor. Unlike the flexible scales possessed by many fishes, poachers are encased in rigid plates that overlap in rows. Uniquely, when viewed in the hoop direction, rows appear as distinct geometric rings which can be dissected out both digitally and physically. These rings vary across species in both number and arrangement of plates, forming octagons, hexagons, and squares. The diversity in row count and overlap across species implies different ring designs may be specialized for different functions. To test this, we 3D-printed models of poacher armor rings as regular polygons with flexible joints at either the center or corners, varying the number sides to match the diversity seen in nature. We used a material testing system to compress the models to a locking position, recording force displacement curves for each model. We found that, across most shapes, models with central joints, which most closely match poacher scale morphology, require more force to reach a locked position than models with joints in the corners. This means the models that closely resemble fish, despite being contradictory to conventional engineering design, resist compression better. Poachers are not fast swimmers and thus hide under rocks, compressing themselves, but due to their scales' resistance, they can prevent damage to their soft internal structures.

Introduction

Armor is exceptional amongst fish innovations due to its multitude of different uses. Armor can provide protection from the environment and predators, signal age and

experience, or serve as a visual display for others of the species (Kruppert et al., 2020). In fishes, armor often takes the form of dermal plates: hard, stiff, and enlarged scales that reinforce the body's surface (Chen, Mckittrick, & Meyers, 2012). These plates are made up of extremely mineralized collagen fibers, with fiber density and orientation varying among different clades of fish (Chen, Mckittrick, & Meyers, 2012). Different clades of fishes with armor have varying mechanical adaptations that allow them to be successful, such as energy dissipating nanostructures, multilayering, and reinforced fibrous joints (Song et al., 2011). These mechanical adaptations then dissipate the force from threats, such as bites, in one of three major ways: by deforming or breaking the threat, deforming or breaking the armor, or some combination of both (Song et al., 2011). Across lineages that have evolved armor, its structure is highly morphologically diverse. Some species, such as poacher fish have a high density of interlocking plates whereas others such as the Chinese sturgeon have plates spread out across their body. Others, like boxfishes, have a single, rigid carapace covering their entire body (Yang et al., 2015).

Armor has evolved most frequently in fishes that were previously scaleless. These bony plates are then often permanent evolutionary fixtures, as armor is very rarely lost in the lineage (Lemopoulos & Montoya-Burgos, 2021). Many lineages of extant fishes evolved armor as an adaptation to a benthic lifestyle. This is due to the high proportion of benthic fish being scaleless and thus needing some form of protection and thus evolving the comparatively simpler bony plates rather than scales (Lemopoulos & Montoya-Burgos, 2021). Yet the most iconic examples of armor evolution are its escalation through predator-prey arms races (Song et al., 2011). In order to avoid being eaten, some fishes evolved light armor. Their predators evolved ways around the armor such as larger

teeth and increased biting force; thus, driving the armor to continually increased thickness (Song et al., 2011). A great example of this is *P.senegalus* which over time evolved both thicker armor and larger teeth to both protect from and attack members of the same species (Song et al., 2011).

The morphological diversity of armor facilitates a range of defensive mechanisms. While some armor is punctuated and non-overlapping, like the large conical plates of sturgeons; others are completely overlapped, like in poachers. Such structural variation has dramatic effects on the armor's mechanism of force dispersal. Each non-overlapping plate of the sturgeon is able to resist compression due to its individual ridge-like structure (Zheng et al., 2023). In contrast, poacher scales overlap to form a cohesive ring-like structure where each scale supports those near it (Zheng et al., 2023). When multiple scales are overlapped, if one scale has pressure put onto it, the adjacent scales can help distribute a portion of the force (Funk et al., 2015). However, even with this network of force dispersion, the scales still tend to fail on an individual basis, rather than as a unit, making this a powerful tool for defense (Funk et al., 2015).

One of the most important aspects of armor is the balance between rigidity and flexibility. The more mineralized and encompassing a fish's armor is, the less the fish will be able to move due to the layer of thick plating (Yang et al., 2013). However, if a fish's armor is very low in mineral density or covers very little of the fish, any outside threat such as a predator's teeth, or a rock that is pushed onto the fish, will break through the thin armor and damage the fish (Yang et al., 2013). An effective yet all-purpose armor requires fishes to find a medium between extremely mineralized high coverage armor and thin low coverage armor that achieves both protection and free movement.

Biological armor of all morphotypes is exposed to a diverse suite of force modes in nature. These include concentrated forces from teeth or claws, distributed forces from environmental features like rocky crevices, and abrasive forces from the benthos. Each of these compressive forces tends towards a different failure mode, such as cracking, buckling, or erosion (Song et al., 2011). Here, we focus on buckling, a failure mode in which a structure bends outward and can no longer support a load. Flexibility in armor structures is particularly essential resisting buckling, as flexibility in structural properties can allow the armor, under strain that typically would produce buckling, to bend and deform when compressed in a way that avoids permanent structural damage.

Fishes in the family Agonidae (poachers) have rigid scales covering their entire bodies that are each connected to one another with flexible material (Kolmann et al., 2020). These rigid scales are arranged in a distinct pattern: rather than being spread randomly, their scales form very distinct rings (Figure 1). These rings are arranged in horizontal rows from the head to the tail of the fish, with the number of scales in each ring varying depending on species of and location on the fish. These rings, when viewed as a cross section, create distinct geometric shapes depending on the number of scales in the ring. Rings can have either 4, 6, or 8 scales, which form a shape resembling a square, hexagon, and octagon respectively (Figure 1). This geometric variation presents an opportunity to test how armor shape influences mechanical performance. Poachers vary wildly in the arrangement of their scales. Among poacher species, there is variation in the number of rings on the fish, the mineral density and overlap of each scale, the number of scales per ring, and the shape of rings compared to body location (Figure 1). This raises a question regarding the purpose for differences in scale morphology.

Genus	Species	SPR Behind Head	SPR Between Dorsal Fins	SPR At Tail
Agonopsis	*Vulsa*	8	8	6
Anoplagonus	*Inermis*	6	6	6
Aspidophoroides	*Bartoni*	6	6	4
Aspidophoroides	*Olrikii*	8	8	6
Bathyagonus	*Alascanus*	8	8	6
Bathyagonus	*Infraspinatus*	8	8	6
Leptagonus	*Decagonus*	8	8	6

Figure 1. Number of scales per ring in different poacher species. SPR stands for scales per ring. These counts do not include lateral line scales, as they were not large or dense enough to provide additional protection. In each section each ring has the same number of scales. The sections were from behind the head to the front dorsal fin, between the dorsal fins, and from the rear dorsal fin to the tip of the tail. There is a trend of an 8-8-6 layout.

We observed poachers squeezing underneath rocks as well as being crushed by crabs, two major mechanisms of selection for compressive resistance. In this study, we investigate whether differences in ring geometry alter resistance to buckling, and whether poachers' unusual armor design allows them to maintain both flexibility and compressive strength. We hypothesize that the unique central joint placement and shape will significantly impact the buckling characteristics of these regular polygons due to the novel ways in which the shape will contort when compressed. We predict that shapes with higher numbers of sides will require more force to buckle, as this is the configuration most commonly seen in poachers. We also expect that the shapes with central joints will have a higher resistance to buckling because central joints mirror those of poachers, which need compressive resistance in order to survive. By examining these natural structures, we aim to understand how evolution has solved the challenge of

combining protection with mobility, and how these solutions might inform bio-inspired design. (Figure 2).

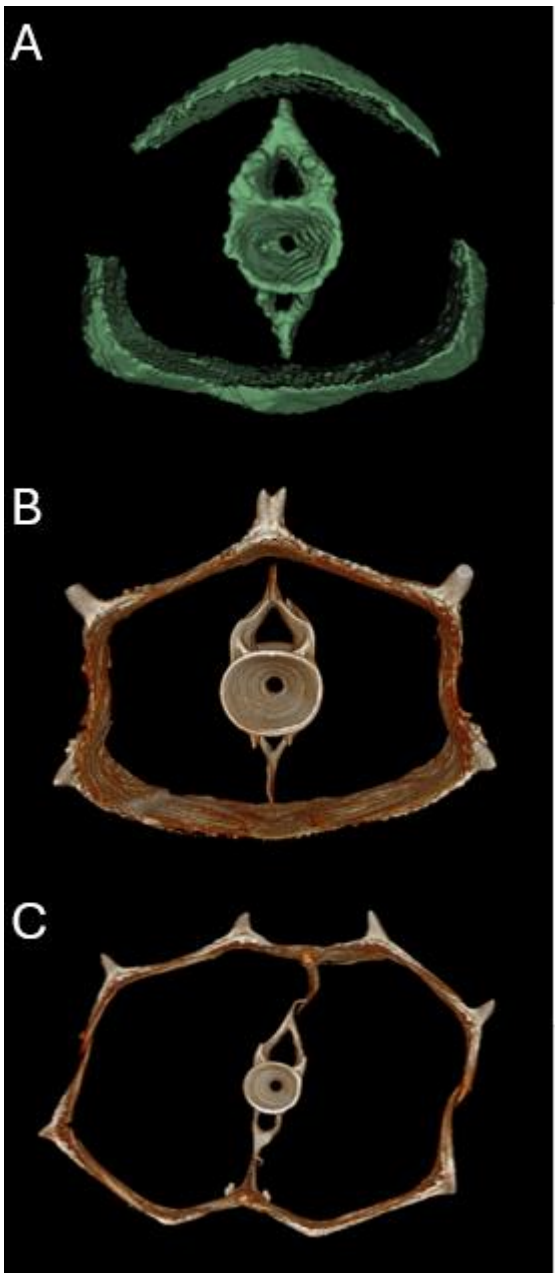

Figure 2. Examples of poacher scale ring layouts. Examples of the 4, 6, and 8 scale ring shapes obtained from microCT-scans. **(A)** An 8-scale octagon shape from the species *A.Bartoni*. (**B)** A 6-scale hexagon shape from the species *B.alascanus*. **(C)** A 4-scale square from the species *B.alascanus.*

Methods

Morphology

We started by investigating the morphology of multiple different species of poachers. We looked at *B.alascanus, A.chiloensis, L.decagonus, A.olrikii,* and *B.infraspinatus* (Figure 3). We used micro-computed tomography (microCT) scans and the software *Slicer* to look at high definition 3-dimensional models of poachers. In doing so we were able to see the distinct interconnected scale rings. We used *Slicer* to segment a single ring of each shape, which allowed us to more closely investigate their structure.

We found that each ring strongly resembled a regular polygon. We then took measurements of the length of each scale as well as the circumference of the scale ring. This allowed us to investigate the dimensions of each scale as well as calculate the overlap of the ring. We also investigated different species of poachers to find how many scales each ring had at different locations on the fish's body.

Genus	Species	kV	uA	Exposure (ms)	Filter
Agonopsis	*Chiloensis*	65	123	1200	Al 1mm
Aspidophoroides	*Olrikii*	65	123	1180	Al 1mm
Bathyagonus	*Alascanus*	90	88	202	Al 1mm
Bathyagonus	*Infraspinatus*	65	123	1180	Al 1mm
Leptagonus	*Decagonus*	65	123	1180	Al 1mm

Figure 3. Specifications of scans used for percent overlap. The specific parameters for each scan used in the analysis of scale overlap.

Modeling

We used a PrusaXL 3D printer to create multiple idealized models that represent singular rings of poacher scales. Each model was printed using a combination of thermoplastic polyurethane (TPU) and polyethylene terephthalate glycol (PETG) filament with TPU being used for the joints and PETG for the rigid structures. Combinations of flexible and inflexible materials allow for partial flexibility similar to that found in poacher scales. We created models of three different shapes (square, hexagon, and octagon) to represent the three different shapes poacher scales are shown to make (Figure 2). The models were standardized by cross sectional area, with each model having a cross-sectional area of 1600mm^2. We chose to standardize by cross-sectional area to allow for simple stress calculations and we chose 1600mm^2 because it is large enough to see the shapes deformations clearly. The models each have a 4mm long joint at either the corners, or in the center of the beams (Figure 4). These joints were printed with an interfacing method that alternates layers of each material when printed, allowing for better connectivity and a lower chance of the different materials shearing. The 4mm length allows for a large joint to still be present even with the material used for interfacing. The models were each 2mm thick and 20mm deep, both of which are similar proportions to poacher armor (Figure 4).

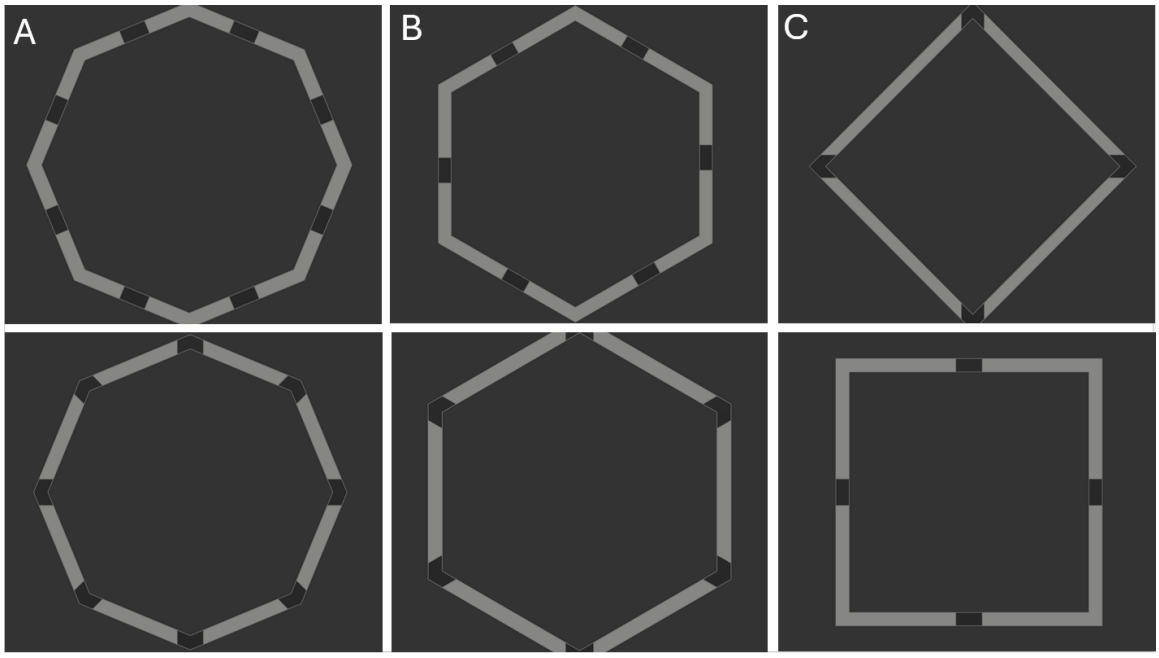

Figure 4. Poacher Scale Ring Models. A top-down view of the model poacher scale rings. The darker black sections are flexible joints made of TPU, and the lighter gray sections are hard and made of PETG.

Materials Testing

In order to test the buckling properties of these poacher ring analogs, we put them through compression tests, with plates, the plates represent being crushed by a large object such as a rock. The compression tests were performed on an MTS machine (Figure 5). The plates were flat and 3d printed using PETG. They were then attached to the MTS machine and were pushed together until the designated materials threshold.

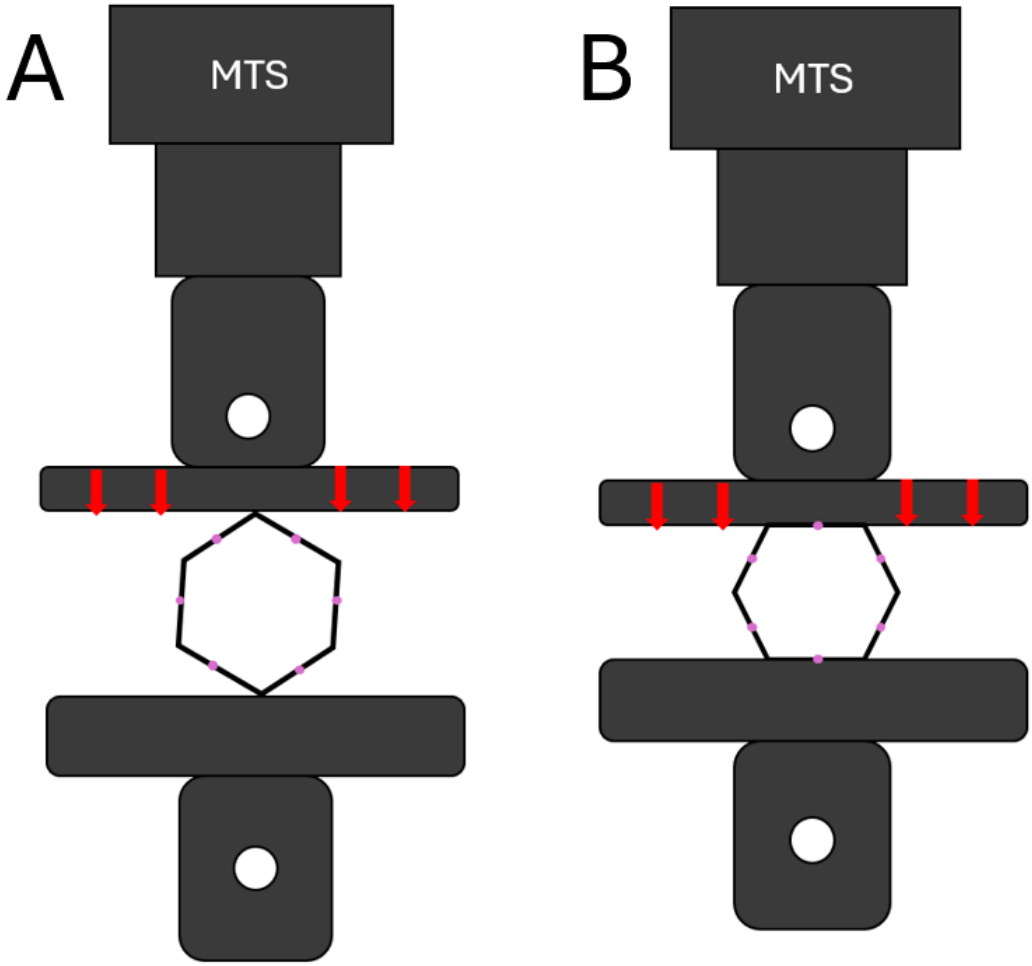

Figure 5. Model of MTS Machine Used to Compress Scale Ring Models. Arrows denote direction of plate motion. Pink dots are joints on the scale ring model. Circle holes in MTS are where pegs are inserted to secure plates. **(A)** Model is being compressed on its edge. **(B)** Model is being compressed flat.

To determine the distance needed to compress we identified the buckling configuration of the shapes. We define the buckling configuration as the shape in which the models begin to buckle when compressed. This is usually created by direct contact with a purely rigid structure and the plate. For example, an octagon with soft corners turns into a rectangle when compressed and thus can begin to buckle due to the rigid vertical beams coming into contact with the plates (Figure 6.

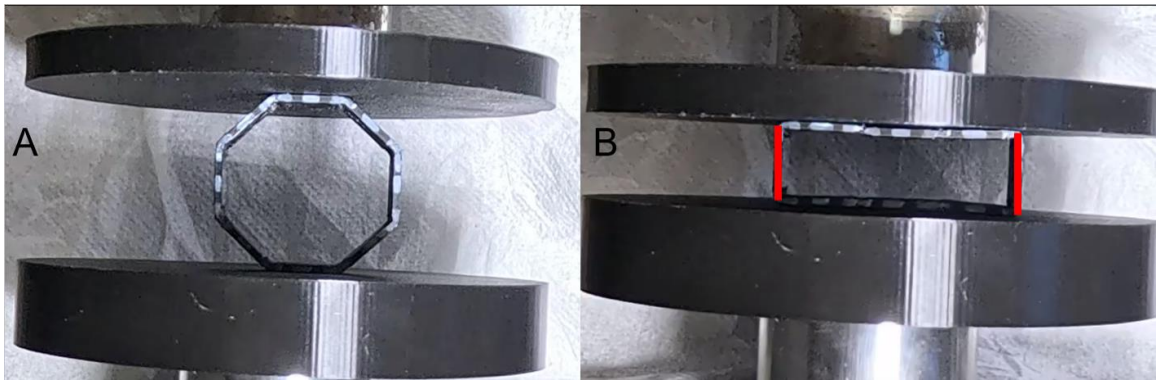

Figure 6. Example of Buckling Configuration. An example of an octagonal model with corner joints in **(A)** its initial position and **(B)** its buckling configuration. Red lines represent rigid sections in contact with plates.

We calculated the distance we would need to compress to reach this buckling configuration by finding how far the model would need to be compressed until a mostly vertical rigid structure was created. This was often the point where the plates came into contact with both sides of a single rigid section with no flexible section in between. We then continued to compress the model a further 0.5mm to ensure the truly reached buckling. This method of compressing to the point just before buckling begins allows us to avoid simply testing the strength of PETG but rather the unique characteristics of these shapes. Some shapes did not have a configuration in which they buckled or would begin to buckle immediately upon compression. If the shape did not have a buckling configuration, we compressed it as far as the MTS would go. If the shape started in a buckling configuration, we compressed it to 5mm to get a reasonable amount of data. Each shape and joint combination had three compression tests run on it, using three separately printed replicates of each model to account for errors in the 3D printing. The models were compressed both flat, such as in Figure 6A, and on their corner.

Data Analysis

The first way in which we analyzed this data was by looking at the force required to reach 5% and 10% strain, the measure of change in cross-sectional area. We then did an ANOVA to test for any significant difference between the values. When the force values are compared, we can find what shapes, joint placements, and orientations take the most force to compress. We also looked at the slope of the load extension curve created by the MTS at 2% strain. A load extension curve describes how much force is required to move the MTS plate a certain distance. We chose 2% strain because our data created unreasonable results due to outliers at higher strains and 2% is enough to have meaningful deformation without including the outliers. This data gives us further insight into the force required to compress the models as well as giving additional information on how quickly the load increased. We also measured the percent overlap of multiple different scale rings, comparing the overlap of scales from both octagonal and hexagonal rings from microCT scans. This gives us information on possible inaccuracies of the models as well as possibly unseen morphological differences in different types of scale rings.

Results

Joint Placement Load*:* We found that when compressed to both 5% and 10% strain, there was a significant difference in the load required to compress squares with central joints and squares with corner joints. This was true regardless of the orientation in which the squares were compressed. When compressed on their edge to 5% and 10% strain, on average, 10.453N and 2.406N more, respectively, were required to compress the square models with central joints than the square models with corner joints. When compressed

flat, to 5% and 10% strain, on average, 137.273N and 229.348N more, respectively, was required to compress the square models with corner joints. In hexagon models, at 5% strain there was no significant difference between joint placements when compressed on their edge. However, the hexagon with center joints took an average of 2.735N more to compress when flat. At 10% strain there was no significant difference between either joint placement in hexagons. At both 5% and 10% strain and when compressed both on its edge and flat the octagon with central joints always required significantly more force to compress than the octagon with corner joints. That being, on average, 2.269N and 3.019N when compressed flat to 5% and 10% strain respectively and 1.425N and 2.462N when compressed on its edge to 5% and 10% strain respectively. (Figure 7)

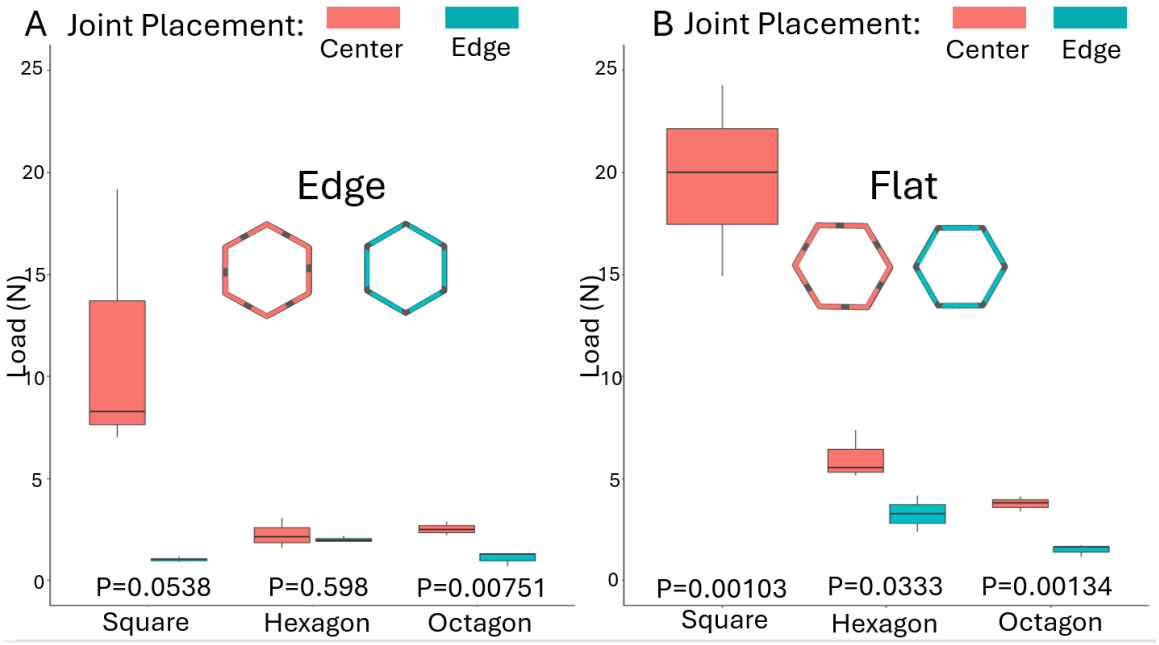

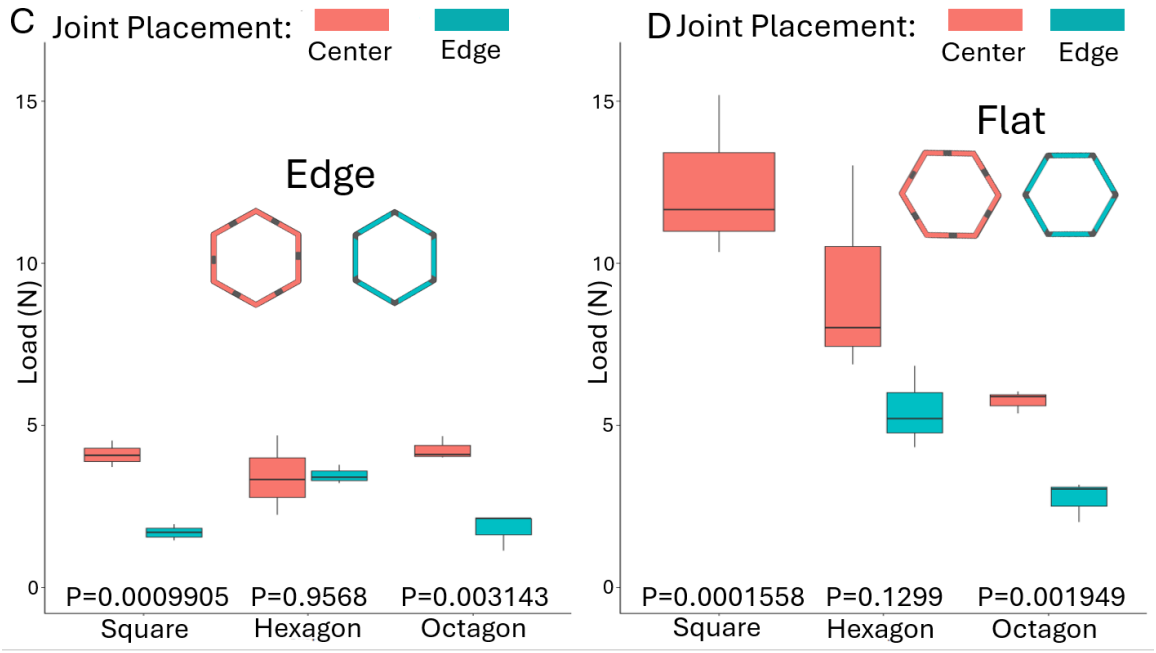

Figure 7. Load at 5% and 10% strain. Plots A and B are of load at 5% strain and Plots of C and D are of load at 10% strain. Plots on the left are compressed on their edge and plots on the right are compressed flat. Square with corner joints is not depicted due to its unique structure starting in a buckling position and thus causing extremely high force values. (**A)** Squares and octagons with center joints required more force to compress (Sq P=0.0538, Oct P=0.00751). **(B)** Squares with corner joints required more force to compress (P=0.00103) whereas in hexagons and octagons more force was required to compress the shapes with center joints (Hex P= 0.0333, Oct P=0.00134). **(C)** Squares and octagons with center joints required more force to compress (Sq P=0.000991, Oct P=0.00314). **(D)** Squares with corner joints required more force to compress (P=0.000156) whereas in octagons more force was required to compress the shapes with center joints (P=0.00195).

Slopes: We found that in squares when compressed on both their edge and flat that at 2% strain, the models with center joints had a significantly higher slope on their load displacement curve. In all instances with hexagons, there was no significant difference between different joint placements. In octagons compressed both on their edge and flat,

the slope of the load displacement curve was significantly higher in shapes with center joints.

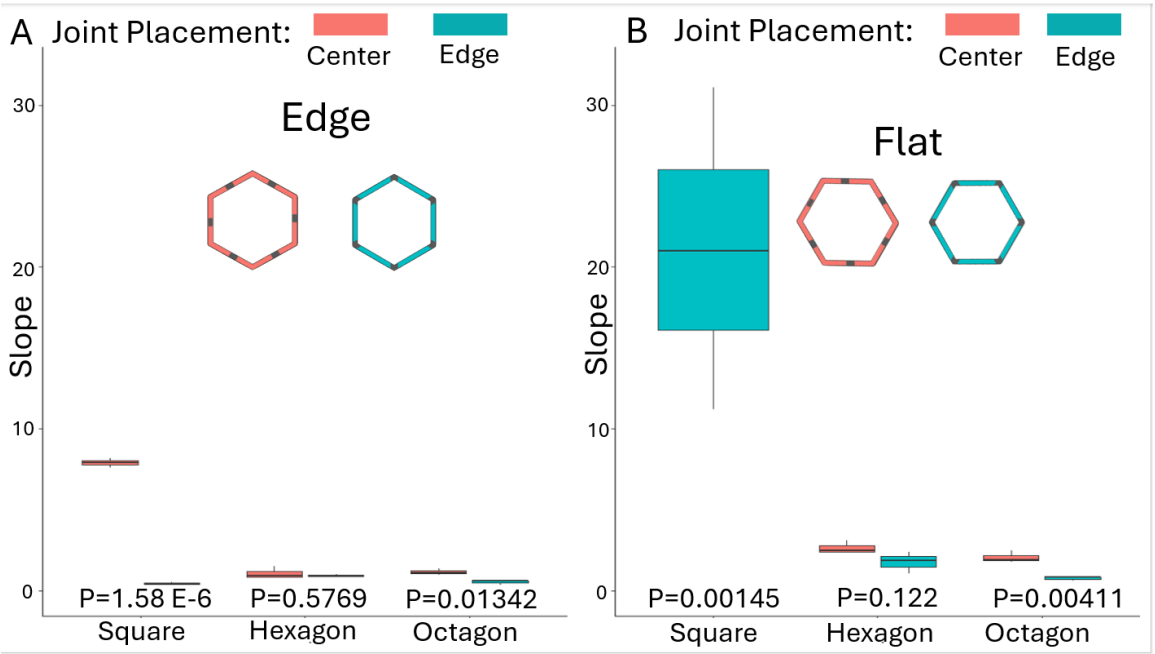

Figure 8. Slope of load displacement curve at 2% strain. Plots on the left are compressed on their edge and plots on the right are compressed flat. Square with central joints is not depicted due to its unique structure causing extremely high force values. **(A)** Squares and octagons with central joints required more force to compress (Sq P=1.58 E-6, Oct P=0.01342) **(B)** Squares and octagons with central joints required more force to compress (Sq P=0.00145 E-6, Oct P=0.00411).

***Percent Overlap*:** We found when measuring the overlap of scales across multiple species of poachers that there is no significant difference between the percent overlap of hexagonal and octagonal scales. The average percent overlap for octagonal scales was about 11% and the average percent overlap for hexagonal scales was about 16%.

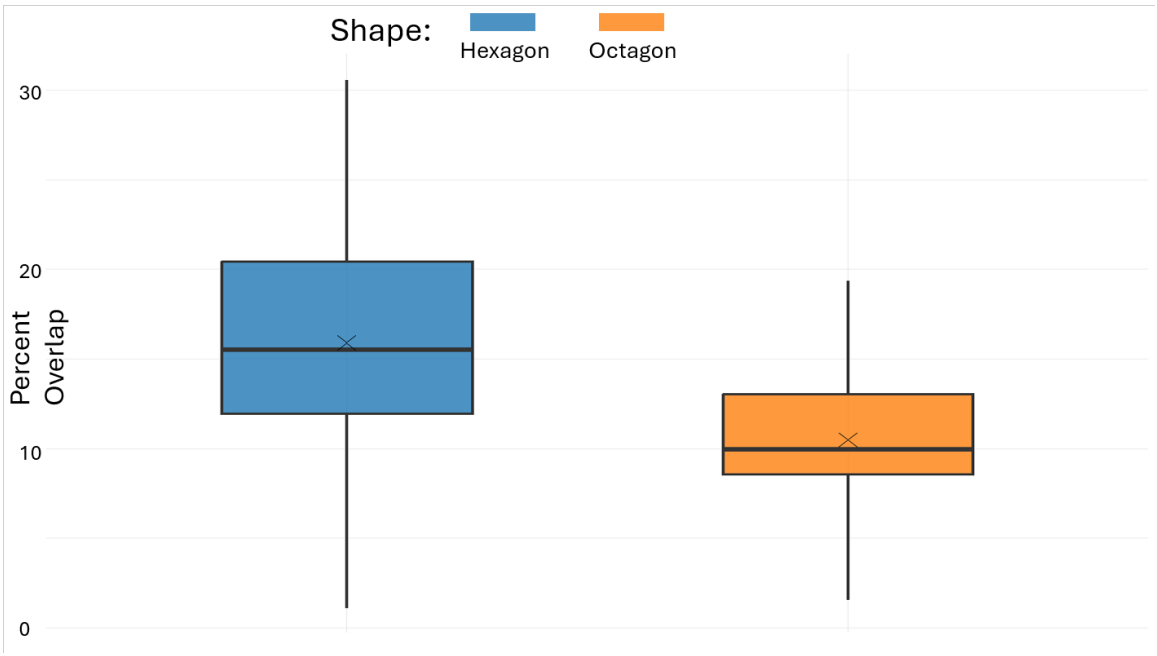

Figure 9. Percent Overlap of Different Shapes. Shows the difference in percentage overlap between hexagonal and octagonal scale rings. There is no significant difference.

Discussion

Compression Resistance: One of our most interesting results is that, in certain shapes and orientations, central joints enhance resistance to compressive forces. Across multiple compression levels, octagons with central joints required greater force to compress than those with corner joints. We found similar patterns in square models oriented on their edge, and in flat hexagons at lower compressive forces. These results suggest that the ability of poachers to thrive in high pressure environments, like squeezing in between rocks, may be partly due to their compressive-resistant scale architecture. They can take more force from things like rocks and predators and come out unscathed due to their armor and specifically the joint placement in their armor helping to absorb the force.

may be partly due to their compressive-resistant scale architecture.

However, not all shapes behaved as expected, revealing nuances in how structural geometry affects mechanical performance. For example, our square model with corner joints appeared to resist compression more strongly than the square with central joints. We hypothesize that this pattern was not due to an extreme amount of compressive resistance but instead reflects how the joint locking position of this shape occurs immediately upon compression. It takes nearly zero newtons of force to compress the square with corner joints to the locking position.

These findings also raise interesting possibilities for how structural principals of poacher scale biology could be further applied to engineering systems. Compression resistant joint configurations could inspire the development of stronger, more durable burrowing robots or machines capable of maneuvering through rocks or tight spaces. Future work should focus on testing more anatomically realistic models to evaluate these ideas further. For instance, poacher musculature and internal organs could be represented with foam inserts, and the vertebral column simulated with a central beam. The overlap of poacher scales is also very complex, we represented it here with large joints, but it could be shown with a more complex overlapping plate design. Comparing compression responses in these refined models would reveal whether the patterns identified here persist under more realistic conditions. This would allow for an even better look as to how this may be applicable in robotics. Since many robots also have dense internals, adding these to the models to see how they affect compression could prove extremely useful.

Morphological Implications: Our findings also revealed how specific scale shapes and orientations contribute to mechanical stability and resistance to buckling. Among shapes with central joints, the octagon does not buckle when compressed flat, nor does the hexagon when compressed on its corner. This is particularly interesting given that many species of poachers, such as *Bathyagonas alascanus* and *Agonopsis vulsa,* display scale ring layouts consisting of flat octagons along the first two thirds of their body and corner-oriented hexagons posteriorly. This arrangement likely confers near-total buckling resistance, suggesting an optimized pattern for mechanical stability that has evolved across multiple taxa.

Variation among species indicates that scale architecture may reflect different ecological pressures or evolutionary histories. Some species, such as *Anoplogmis inermis,* possess flat hexagonal plates across their entire body, implying an alternate functional emphasis with reduced reliance on compressive resistance. To explore these differences, future work would incorporate a phylogenetic analysis of *Agonidae* fishes. This would assess whether armor variation reflects shared ancestry or environmental adaptation. If many poachers that live in similar environments have similar scale patterns, then that would lend credence to the idea that the specific ring shapes and orientations serve distinct mechanical roles in response to ecological pressures.

Bibliography

Alexandre Lemopoulos, Juan I. Montoya-Burgos, From scales to armor: Scale losses and trunk bony plate gains in ray-finned fishes, *Evolution Letters*, Volume 5, Issue 3, 1 June 2021, Pages 240–250,

Funk, N., Vera, M., Szewciw, L. J., Barthelat, F., Stoykovich, M. P., & Vernerey, F. J. (2015). Bioinspired Fabrication and Characterization of a Synthetic Fish Skin for the Protection of Soft Materials. *ACS Applied Materials & Interfaces*, *7*(10), 5972–5983.

Kolmann, M. A., Peixoto, T., Pfeiffenberger, J. A., Summers, A. P., & Donatelli, C. M. (2020). Swimming and defence: Competing needs across ontogeny in armoured fishes (Agonidae). *Journal of The Royal Society Interface*, *17*(169), 20200301.

Kruppert S, Chu F, Stewart MC, Schmitz L, Summers AP. Ontogeny and potential function of poacher armor (Actinopterygii: Agonidae). Journal of Morphology. 2020; 281: 1018–1028.

Po-Yu Chen, Joanna McKittrick, Marc André Meyers, Biological materials: Functional adaptations and bioinspired designs, Progress in Materials Science, Volume 57, Issue 8, 2012, Pages 1492-1704, ISSN 0079-6425,

Song, J., Ortiz, C., & Boyce, M. C. (2011). Threat-protection mechanics of an armored fish. *Journal of the Mechanical Behavior of Biomedical Materials*, *4*(5), 699–712.

Yang, W., Chen, I.H., Gludovatz, B., Zimmermann, E.A., Ritchie, R.O. and Meyers, M.A. (2013), Natural Flexible Dermal Armor. Adv. Mater., 25: 31-48.

Yang, W., Naleway, S. E., Porter, M. M., Meyers, M. A., & McKittrick, J. (2015). The armored carapace of the boxfish. *Acta Biomaterialia*, *23*, 1–10.

Zheng Y, Li X, Liu P, Chen Y, Guo C. The Armor of the Chinese Sturgeon: A Study of the Microstructure and Mechanical Properties of the Ventral Bony Plates. *Micromachines*. 2023; 14(2):256.